

AD-A050 122

NAVAL RESEARCH LAB WASHINGTON D C
LONG-RANGE HOLOGRAPHY FIELD EXPERIMENTS.(U)
OCT 77 J A BLODGETT, R L EASTON, R E KONCEN

F/G 14/5

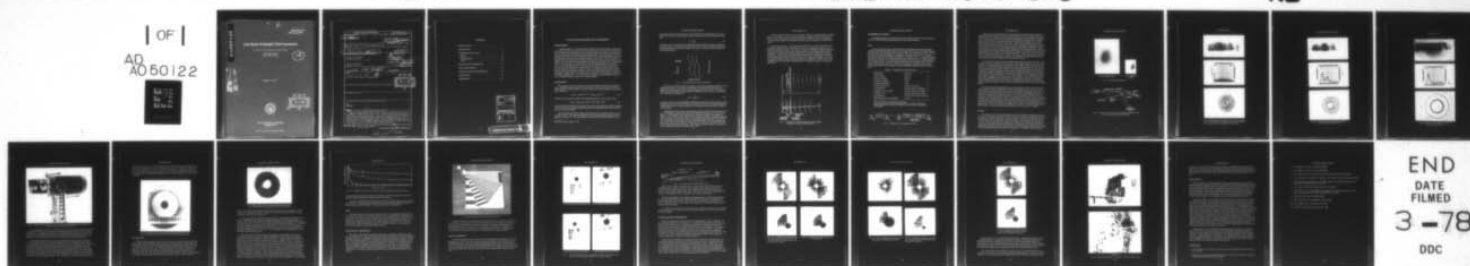
UNCLASSIFIED

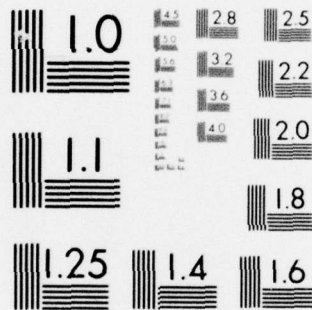
NRL-8167

SBIE-AD-E000 103

NL

| OF |
AD
A050122





MICROCOPY RESOLUTION TEST CHART
NATIONAL BUREAU OF STANDARDS-1963-A

AD A 050122

ade000103
NRL Report 8167

Long-Range Holography Field Experiments

J. A. BLODGETT, R. L. EASTON, Jr., and R. E. KONCEN

*Applied Optics Branch
Optical Sciences Division*

12

AD No. —
DDC FILE COPY

October 31, 1977



DDC
RECEIVED
FEB 17 1978
B

NAVAL RESEARCH LABORATORY
Washington, D.C.

Approved for public release; distribution unlimited.

SECURITY CLASSIFICATION OF THIS PAGE (When Data Entered)

| REPORT DOCUMENTATION PAGE | | READ INSTRUCTIONS BEFORE COMPLETING FORM |
|---|-----------------------|--|
| 1. REPORT NUMBER 14 <u>NRL 8167</u> | 2. GOVT ACCESSION NO. | 3. RECIPIENT'S CATALOG NUMBER |
| 4. TITLE (and Subtitle) 6 <u>LONG-RANGE HOLOGRAPHY FIELD EXPERIMENTS</u> | | 5. TYPE OF REPORT & PERIOD COVERED 9 <u>Final report, one phase of a continuing NRL Problem</u> |
| 6. AUTHOR(s) 10 <u>J. A./Blodgett, R. L./Easton, Jr. R. E./Koncen</u> | | 6. PERFORMING ORG. REPORT NUMBER |
| 7. PERFORMING ORGANIZATION NAME AND ADDRESS Naval Research Laboratory Washington, DC 20375 | | 8. CONTRACT OR GRANT NUMBER(s) 16 <u>RR01147</u> |
| 11. CONTROLLING OFFICE NAME AND ADDRESS Office of Naval Research Arlington, VA 22217 | | 10. PROGRAM ELEMENT, PROJECT, TASK AREA & WORK UNIT NUMBERS 17 <u>NRL Problem N01-16 Project RR01147</u> |
| 14. MONITORING AGENCY NAME & ADDRESS (if different from Controlling Office) 18 <u>SBIE</u> 19 <u>AD-E000103</u> | | 12. REPORT DATE 11 <u>31 Oct 77</u> |
| 16. DISTRIBUTION STATEMENT (of this Report) Approved for public release; distribution unlimited | | 13. NUMBER OF PAGES 12 <u>25P.</u> |
| 17. DISTRIBUTION STATEMENT (of the abstract entered in Block 20, if different from Report) | | 15. SECURITY CLASS. (of this report) UNCLASSIFIED |
| 18. SUPPLEMENTARY NOTES | | 15a. DECLASSIFICATION/DOWNGRADING SCHEDULE |
| 19. KEY WORDS (Continue on reverse side if necessary and identify by block number) Laser Holography | | |
| 20. ABSTRACT (Continue on reverse side if necessary and identify by block number) Active holographic and conventional imaging techniques were compared, with the images for both cases taken simultaneously at a range of 1 km. A 1-joule Q-switched ruby laser with a 1-m coherence length was used as the light source. To obtain both a conventional image and a holographic interference pattern simultaneously through one aperture, a beamsplitter and two cameras were mounted at the focus of a 36-cm-diameter telescope. Tests were conducted for several weeks, involving 257 exposures. At best, holographic imaging showed an improvement in resolution over conventional imaging by a factor of 2 but with a decrease in signal-to-noise ratio. | | |

DDC
RECEIVED
FEB 17 1978
B

DD FORM 1 JAN 73 1473

EDITION OF 1 NOV 65 IS OBSOLETE
S/N 0102-LF-014-6601

SECURITY CLASSIFICATION OF THIS PAGE (When Data Entered)

251 950 JOB

CONTENTS

| | |
|------------------------------------|----|
| INTRODUCTION | 1 |
| BACKGROUND | 1 |
| EXPERIMENTAL DETAILS | 4 |
| Laser | 4 |
| Receiver | 5 |
| Recording Media | 11 |
| Target | 13 |
| PRELIMINARY EXPERIMENTS | 13 |
| FIELD EXPERIMENTS | 14 |
| RESULTS OF FIELD EXPERIMENTS | 16 |
| CONCLUSIONS | 21 |
| REFERENCES | 21 |

| | | |
|---------------------------------|---------------|-------------------------------------|
| ACCESSION for | | |
| NTIS | White Section | <input checked="" type="checkbox"/> |
| DDC | Bull Section | <input type="checkbox"/> |
| UNANNOUNCED | | <input type="checkbox"/> |
| JUSTIFICATION | | |
| BY | | |
| DISTRIBUTION/AVAILABILITY CODES | | |
| Dist. | AVAIL. | and/or SPECIAL |
| A | | |

LONG-RANGE HOLOGRAPHY FIELD EXPERIMENTS

INTRODUCTION

In 1966 Goodman et al. [1] suggested a technique for imaging through a random medium using wavefront reconstruction. Significant improvement in resolution of the reconstructed image over that obtained with conventional imaging techniques was demonstrated using a local wavefront distortion near the imaging system. This topic received considerable attention [2-5] and was experimentally tested at short ranges and finally over a 12-km horizontal path using a 91-cm Cloudcroft telescope as receiver [6]. These experiments suggested that an improvement in terrestrial imaging was possible with this technique, even though it is most suited for imaging satellites through the atmosphere from a ground-based station. The results were inconclusive for horizontal imaging through the atmosphere, since no direct comparison with conventional active imaging (in which a laser source is provided for target illumination) was attempted. The experiment described here was a direct simultaneous comparison of active conventional imaging and holographic imaging through a horizontal turbulent atmospheric path. The results indicate that in most cases holographic imaging results in an improvement in resolution of approximately a factor of 2 but with increased noise. As in the earlier experiments, the main limitation appears to be in the limited dynamic range of the recording medium.

BACKGROUND

The basis for the expected improvement from holographic imaging is the following. For an aberrating medium near the receiver (Fig. 1), the reference wave $R(x,y)$ and the object wave $O(x,y)$ both experience the same aberration; and the amplitude at the receiver can be written as

$$A(x,y) = R(x,y) e^{jW(x,y)} + O(x,y) e^{jW(x,y)}, \quad (1)$$

where $W(x,y)$ represents the effect of the aberrating medium. The intensity is then

$$I(x,y) = |A(x,y)|^2 = |R|^2 + |O|^2 + R^*O + RO^*, \quad (2)$$

so that the interference pattern recorded at the receiver is the same as would be recorded with no aberration. Thus the reconstruction from the hologram should be free of aberrations due to the atmosphere.

The conditions under which image improvement can be expected can be seen in the top half of Fig. 2. The object and reference are two mutually coherent point sources separated by a distance δ . The linear dimension across the wavefront emerging from the

aberrating medium for which the error is much less than λ is represented by Δ . The reference and object waves pass through nearly identical portions of the distorting medium when

$$\delta < \frac{L}{Z} \Delta, \quad (3)$$

which for a given Δ holds when the distorting medium is sufficiently near the receiver. The distortions of both waves are the same when this condition is satisfied; therefore the interference pattern at the detector plane is the same as it would have been without the phase-distorting layer.

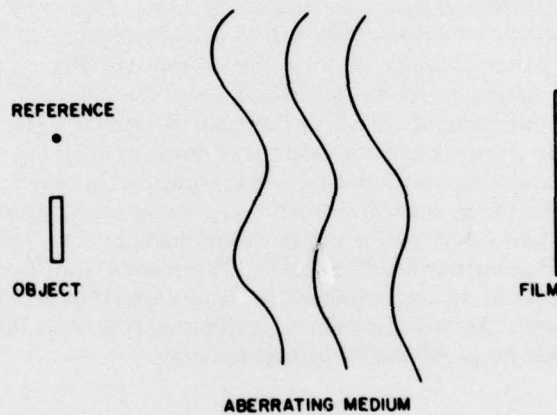


Fig. 1 — Holography through an aberrating medium

This can be contrasted with the situation for conventional imaging represented in the bottom half of Fig. 2. In this case the resolution of the system is nearly that of a diffraction-limited telescope with an effective aperture given by the size of the region Δ measured at the aberrating medium and then projected onto the telescope entrance aperture. This effective aperture is

$$D_{eff} = \frac{L}{L-Z} \Delta. \quad (4)$$

In contrast with Eq. (3) for holographic imaging, which indicates that the effect on image resolution is least when the layer is near the receiver, Eq. (4) for conventional imaging indicates that the effect on image resolution of a turbulent layer is least when the layer is near the object.

Gaskill[3] has shown that for homogeneous, isotropic turbulence the short-exposure case of holographic imaging yields results with diffraction-limited resolution near the reference. As the distance of the object from the reference increases, the resolution decreases to a final value 2/3 that obtained with conventional imaging. Experimental studies were performed to determine the size of the isoplanatic region (that part of the field of view over which the point-spread function remains invariant) for the time averaged case. For an 86-m path this was found to be about 50 mm or less, and for a 542-m path this was reduced to approximately 20 mm. These figures represent averages for a number of tests on different days; each test lasted about 1 min.

For short exposures (less than 10 ms) a larger variation of the data might be expected. Thus it is impossible to predict whether holographic imaging would provide improved resolution over conventional active imaging for horizontal paths through the atmosphere. The experiments at NRL were designed to provide a direct comparison of the two techniques.

As has been pointed out by Goodman and Lehman [7], a serious limitation of the holographic technique is the limited dynamic range of photographic emulsions used to record the interference fringes. This can be overcome by substituting electronic detectors with a greater linear dynamic range, digitally processing the photographically recorded holograms to extend the linear range, or choosing an optimum emulsion-and-developer combination to match the expected amplitude variations due to atmospheric turbulence. The third approach was the one chosen because of the equipment available. This is not the optimum solution, however, since this means the hologram is recorded with a lower contrast than would otherwise be desirable, with a consequent decrease in the signal-to-noise ratio.

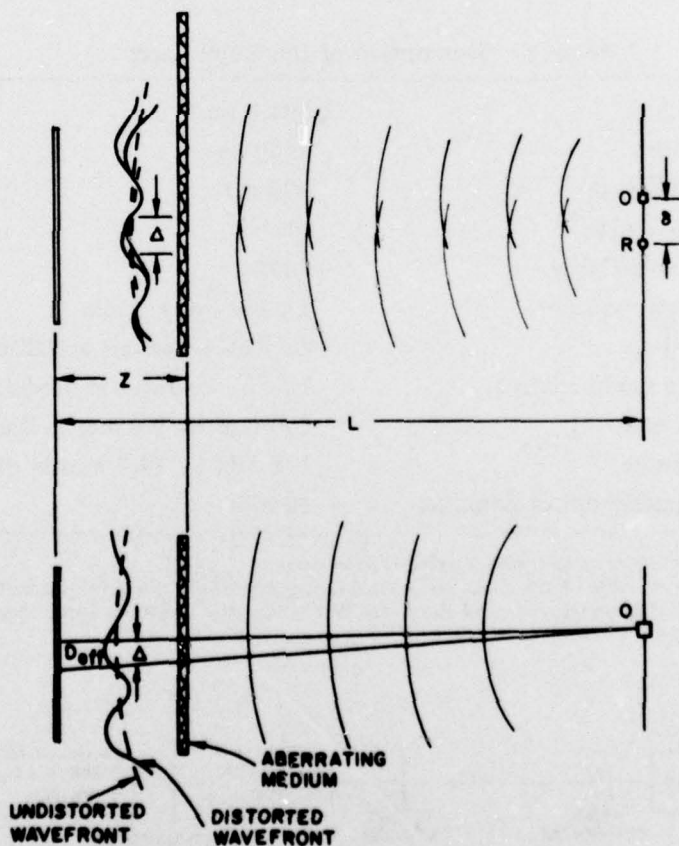


Fig. 2 — Conditions for image improvement by (top) holographic imaging and (bottom) conventional imaging

EXPERIMENTAL DETAILS

The following subsections describe the various components used for the field tests as well as for initial laboratory tests performed to check their operation.

Laser

The laser selected for these experiments was a Q-switched ruby system having an energy of approximately 500 mJ/pulse, a pulse length of 50 ns, and a coherence length of 2 m (Table 1). The wavelength of the ruby laser, 694.3 nm, limited the selection of useful films; nevertheless those available are adequate in sensitivity and resolution. The laser employed an oscillator-and-amplifier configuration as shown in Fig. 3. A transverse mode was selected by the use of a 1.5-mm aperture in the oscillator cavity. A longitudinal mode was selected by the use of temperature-tuned etalons for both the front and rear reflectors of the oscillator cavity. The front etalon was at the same temperature as the ruby rod, and the rear reflector was held at a different temperature by a separate water cooler. These measures were found necessary to achieve repeatable results at the given specifications.

Table 1 — Description of the Ruby Laser

| | |
|--------------------------------|-------------------------------|
| Wavelength | 694.3 nm |
| Pulse width* | ≈ 50 ns |
| Energy (TEM ₀₀) | 500 mJ |
| Coherence length† | >2 m |
| Energy repeatability | $\pm 20\%$ |
| Pulse repetition rate | 1 pulse every 2 min |
| Configuration | Oscillator and one amplifier |
| Transverse mode control | 1.5-mm aperture in oscillator |
| Oscillator rod | 100 mm by 9.5 mm in diam |
| Amplifier rod | 178 mm by 14.3 mm in diam |
| Beam diameter out of amplifier | 12 mm |

*May emit multiple pulses with varying separations.

†Approximately 80% of the shots were acceptable; the other 20% exhibited additional longitudinal modes, reducing the fringe-free coherence length to approximately 6 cm typically.

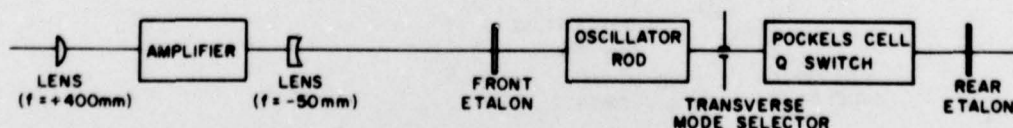


Fig. 3 — Configuration of the holographic ruby laser

NRL REPORT 8167

Extensive tests were performed to confirm that the laser was operating properly. A Fabry-Perot etalon was used to monitor the mode structure for each pulse. These tests were checked in the laboratory by forming off-axis-reference-beam holograms and observing the reconstructions. Secondary modes with energy 10% or less that of the primary modes were found to result in reconstructions with either faint fringes or none at all. Pulse shapes were also recorded for each shot. Typical pulse widths were about 50 ns, but the system frequently emitted two or more pulses with various separations. These extra pulses were due to the slow switching conditions of the Pockels cell Q-switch which were necessary to obtain the long coherence length. The multiple pulses had no effect on the off-axis-reference-beam hologram made in the laboratory, and they did not show up as additional modes as measured by the Fabry-Perot etalon. They were a concern however for the field experiments, since the reference and object must be stationary for the total time the pulses are being emitted. However, no correlation was observed between shots with multiple pulses and holograms which reconstructed poorly.

Another concern was the intensity profile of the beam emitted from the laser. This was not expected to cause any serious problem for the field experiments, since the target would be in the far field; thus any irregularities in the profile would be smoothed, and the effects of turbulence causing breakup of the beam would predominate. For the laboratory experiments, which were conducted in the near field, these nonuniformities would be important, and the expanding telescope used to enlarge the beam from the oscillator through the amplifier was changed. The standard optics employed gave an 8:1 expansion and resulted in a 12-mm-diameter beam out of the amplifier. For the laboratory experiments this was changed to 2:1 expansion at reduced energy. This allowed holography at 30 m with a relatively smooth beam profile. The improvement seen in Fig. 4 is due to reduced diffraction effects from less beam cutoff through the amplifier rod and the fact that the far-field transition has been moved in to approximately 15 m from approximately 200 m.

The other parameter measured for all laser shots was the pulse energy. The energy was measured using an uncoated glass wedge as a beamsplitter at the output of the amplifier and using a photodiode which was frequently recalibrated against a thermopile. To determine the coherence length of the laser, the holographic setup diagrammed in Fig. 5 was used. Off-axis-reference-beam holograms of a 2-m-long target board were taken to allow direct measurement of the depth of reconstruction and thus the coherence length of the laser pulse. Reconstructions of three typical holograms are shown in Figs. 6a, 6b, and 6c along with photographs of the oscilloscope trace from a fast photodiode and photographs of the output of a Fabry-Perot etalon for each example. The photodiode shows the laser output vs time and thus the pulse length and the presence of multiple pulses, if any, and the etalon output indicates the mode structure of the pulse for the hologram.

Receiver

The primary component of the receiver was a 36-cm-diameter Cassegrainian telescope. This was used to form a conventional image directly and was used as a light collector for efficiently recording the hologram. As shown in Fig. 7, a beamsplitter allowed simultaneous recording of the hologram and conventional image. The conventional image was recorded in the usual way, and the hologram was recorded with a camera and 105-mm lens focused on the corrector plate of the telescope. The purpose of the optical system in recording the hologram is to form a reduced image of the interference pattern at the entrance to the telescope and match the energy of the return to the sensitivity of the emulsion.



(a) 2:1 expansion optics



(b) 8:1 expansion optics

Fig. 4 — Laser beam profile at 20 m

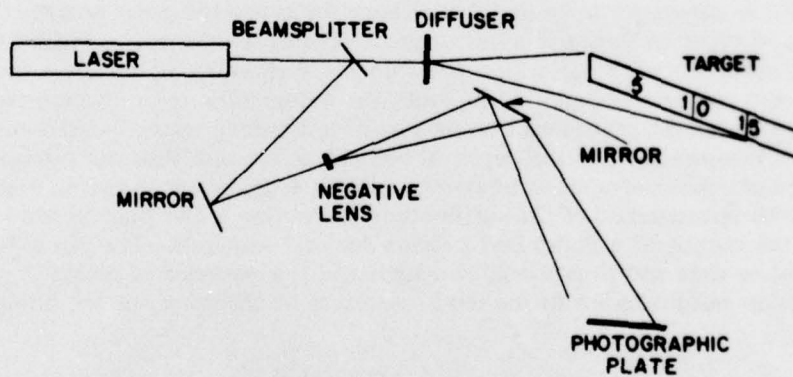


Fig. 5 — Experimental configuration for determining the coherence length of a laser by forming side-reference holograms

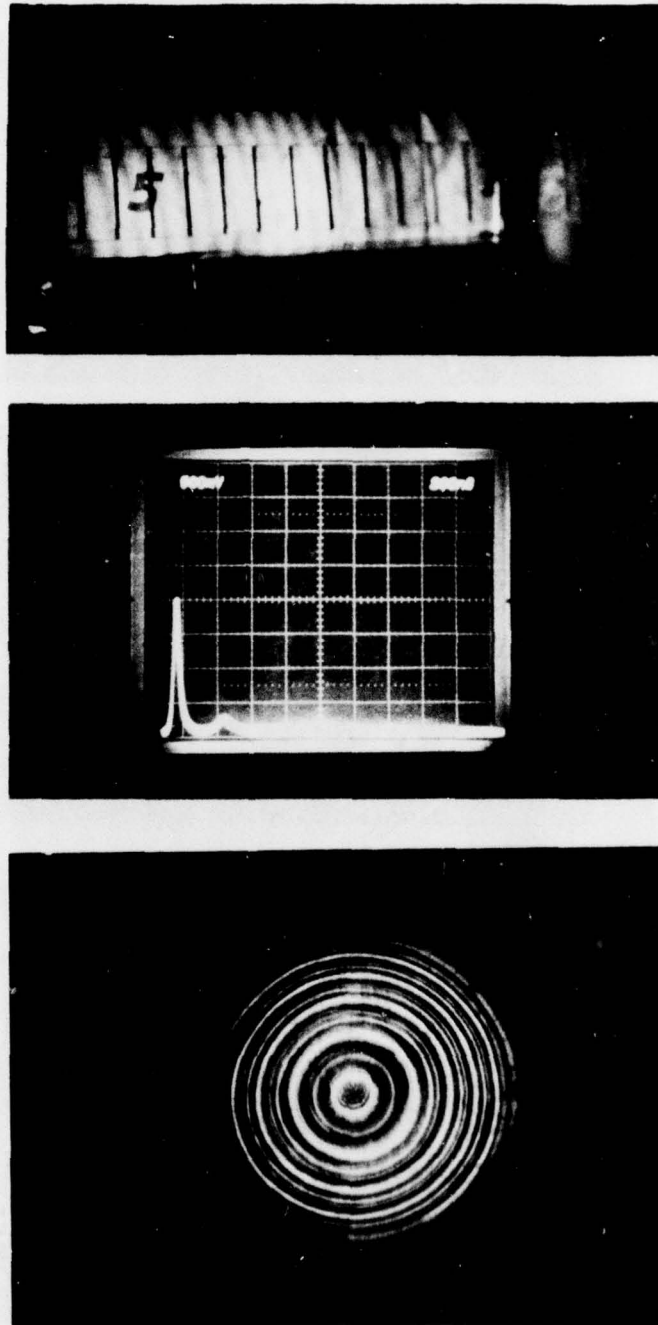


Fig. 6a — Results of a laser coherence test in the case of a double pulse and fine fringes: (top) hologram reconstruction, (middle) pulse profile, and (bottom) Fabry-Perot mode structure.

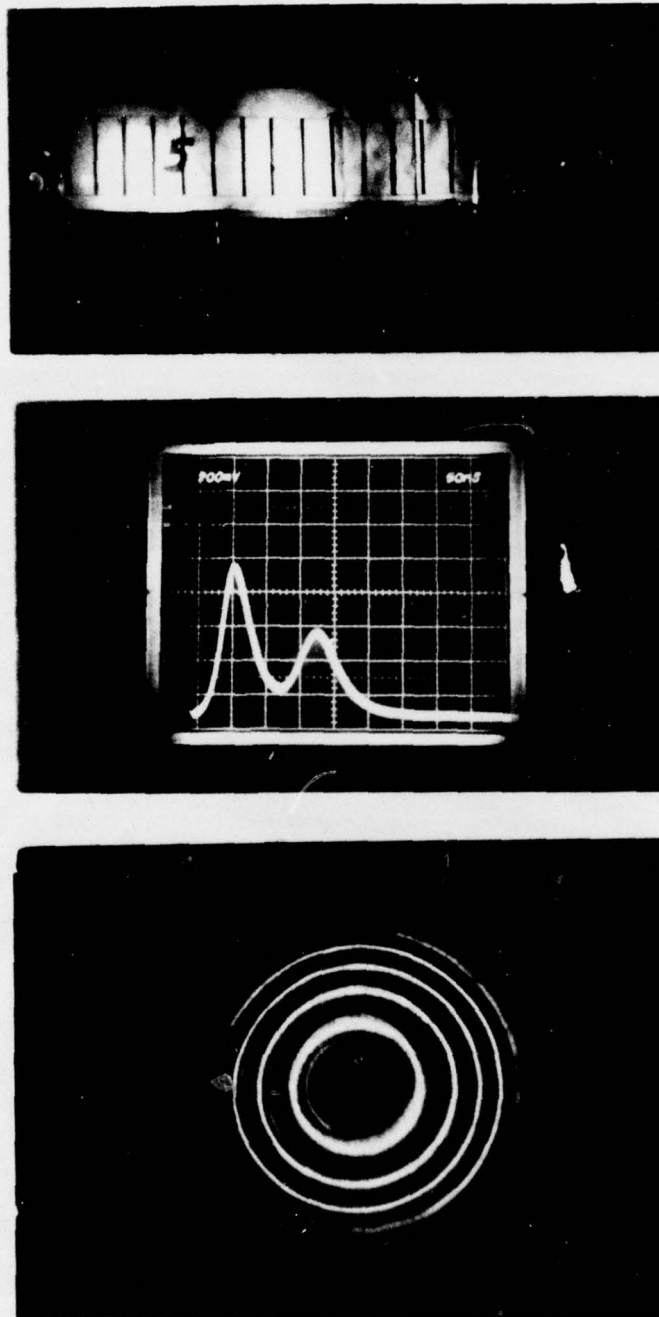


Fig. 6b — Results of a laser coherence test in the case of a double pulse and broad fringes

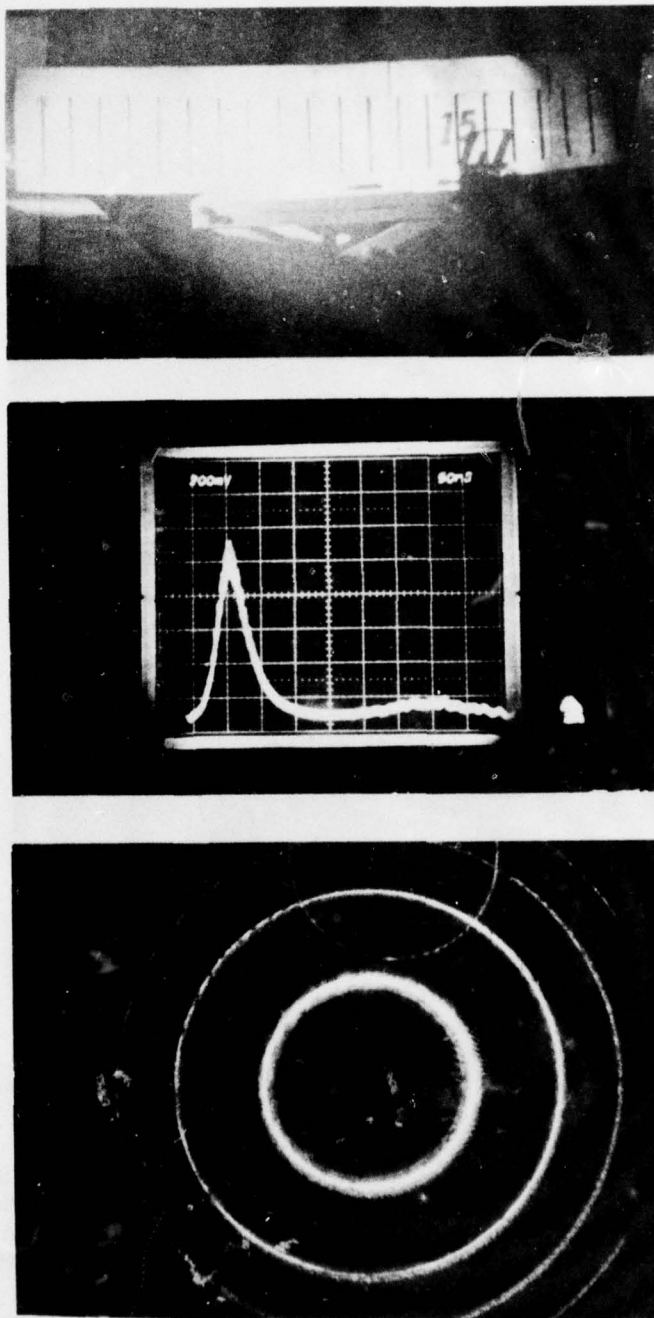


Fig. 6c — Results of a laser coherence test in the case of good reconstruction

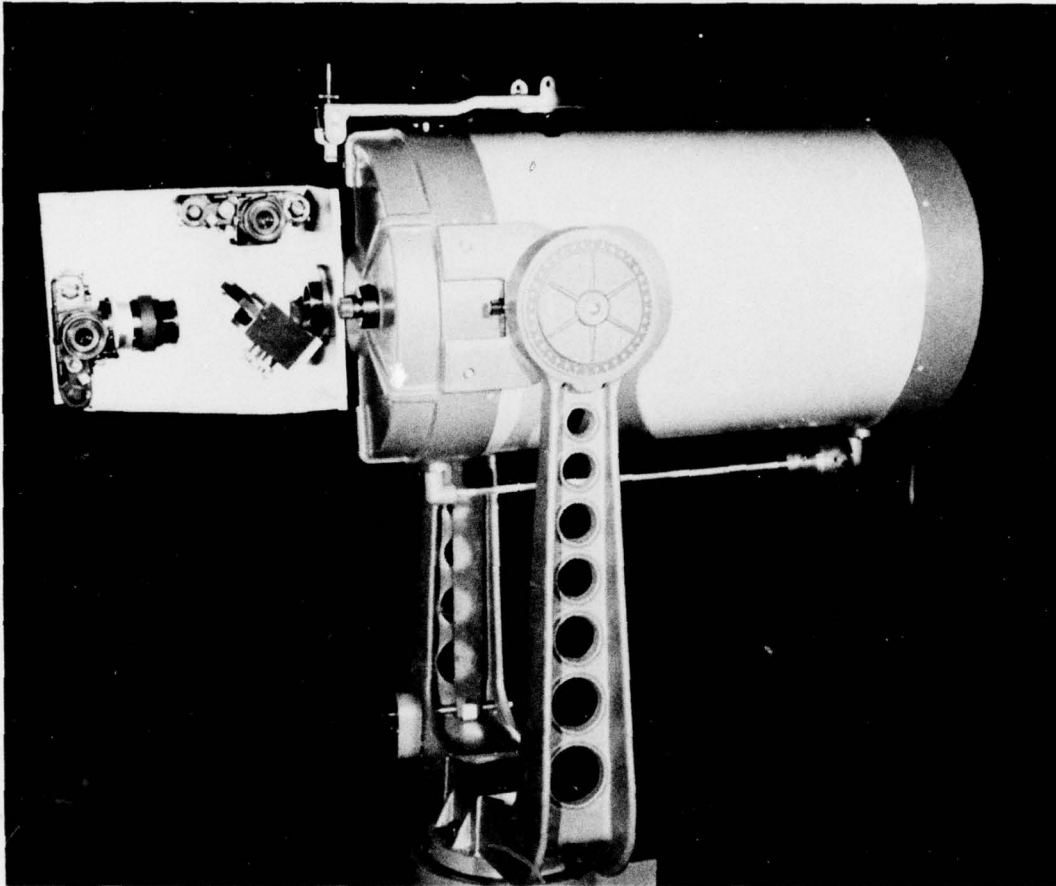


Fig. 7 — Imaging receiver. The upper camera records the conventional image. The camera to the left with the lens records the interference pattern.

The telescope was tested over a 170-m path in an enclosed area to find the resolution in conventional imaging. This resolution was approximately 3 cycles/mm with incoherent illumination. In the field experiments this conventional image was formed from the front reflection off the beamsplitter, which had a surface figure of better than $\lambda/10$; thus no degradation of this image would occur due to the presence of the thick beamsplitter.

The hologram was formed by the beam transmitted through the thick beamsplitter. Such a beamsplitter introduces considerable aberrations in conventional imaging; however in recording holograms these aberrations would be expected to be minimal, since both the object and reference waves undergo the same aberration. This was checked using a Moire technique described by Yokozeki & Suzuki [8]. Holograms were recorded on film using the telescope with plane waves for both the reference and object beams. These holograms consisted ideally of linear sinusoidal amplitude gratings and were made both with and without the thick beamsplitter present. When these holograms were overlaid with a slight offset, Moire fringes were readily observed. Any changes in this interference pattern could be

easily seen. For example, two short exposures, both made without the beamsplitter, resulted in the pattern seen in Fig. 8. The distortions are due to turbulence caused by the air-conditioning blowers in the area. With longer exposures to average these turbulence effects, the patterns obtained are presented in Fig. 9. These show that the effects of the beamsplitter are indeed negligible compared to the residual turbulence in an enclosed environment.

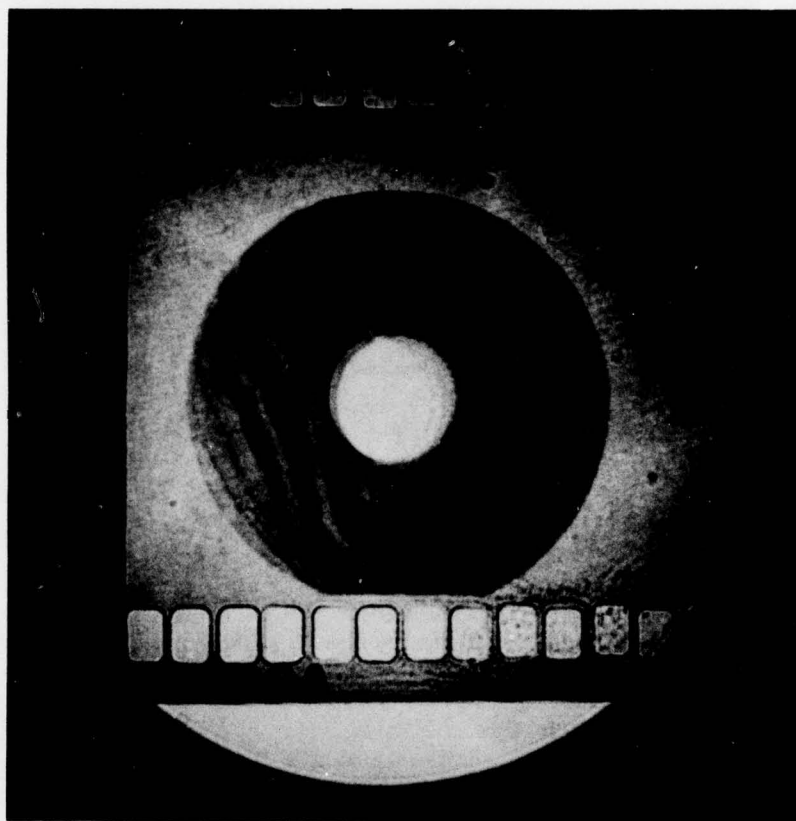


Fig. 8 — Moiré pattern of two short-exposure holograms to determine whether the thick beamsplitter had any effect on the recorded interference pattern

Recording Media

A major problem associated with Goodman's earlier experiments was the limited dynamic range of the photographic film used as the recording medium. Propagation of the laser beams through the turbulent atmosphere imparts a large dynamic range to the intensity variations at the receiver. If a high-contrast emulsion-and-developer combination is used for a high signal-to-noise ratio, then large areas of the hologram are saturated or effectively unexposed. This results in a loss of resolution, a loss of sensitivity, and a spreading of the zero order in the reconstruction of the hologram. The use of an extremely-low-contrast large-dynamic-range recorder at the opposite extreme would extend the

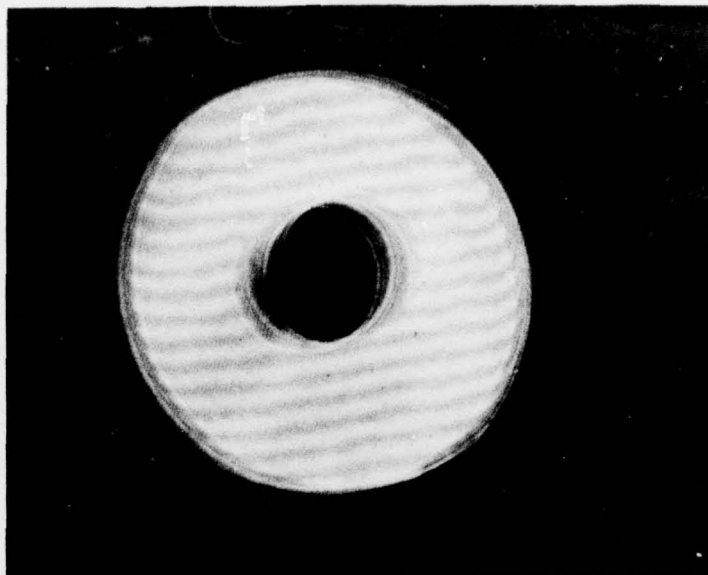


Fig. 9 — Moiré pattern of two long-exposure holograms which averaged the turbulence from air-conditioning blowers that affected Fig. 8

dynamic range so that the hologram is linearly recorded, but this would result in a serious decrease in the signal-to-noise ratio. Both of these combinations were tried in the earlier experiments, with the expected results.

For this experiment a compromise was attempted. Various films and developers were tested in an attempt to determine an optimum combination for the expected degree of turbulence [9]. From the work of Deitz [10] the dynamic range required for linear recording can be estimated. For clear weather, atmospheric attenuation coefficient $\sigma_A \approx 0.15 \text{ km}^{-1}$, and strong turbulence (index structure coefficient $C_n \approx 5 \times 10^{-7} \text{ m}^{-1/3}$), the estimate of the dynamic range required for the recording is about 15 dB. For clear weather with intermediate turbulence ($C_n \approx 4 \times 10^{-8} \text{ m}^{-1/3}$), the estimate of the required dynamic range decreases to approximately 10 dB.

Compromises were found necessary in the selection of an emulsion-and-developer combination for field experiments. Eastman 2496 RAR and 2476 films were chosen because their resolution and spectral sensitivity matched the experimental requirements reasonably well. The holograms as recorded were 10 mm in diameter, which is a linear reduction factor of 36:1. A point source 1 m from the reference at a range of 1 km would produce fringes with a spatial frequency of 50 cycles/mm on the hologram. This is well within the resolution limit of the film [9]; thus 1-m^2 areas can be recorded holographically. Various developers have been tested with this film to achieve the desired dynamic range. Amplitude transmittance versus exposure is shown for 2496 RAR film in Fig. 10 for three developers: D19, D76, and POTA. D19 provides a high-contrast recording which would give optimum signal-to-noise ratio in the reconstructed hologram with low atmospheric turbulence. POTA [11] conversely provides extremely large dynamic range but low contrast. These two combinations are similar to those used in the earlier experiments. It was thought

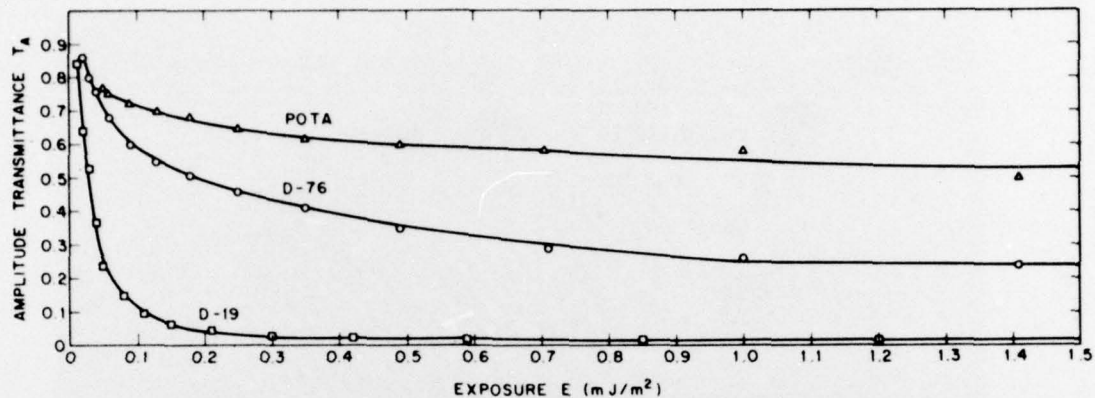


Fig. 10 — Amplitude transmittance vs exposure for Kodak 2496 RAR film and three developers

that the medium-contrast developer D76 would prove a better choice for this experiment; therefore most of the data were taken with this combination.

The choice of 2496 RAR film and D76 developer is not ideal, because of the nonlinear T_A -vs- E curve. As Goodman has pointed out, an electronic detector with greater linear dynamic range would be preferred. Unfortunately this was not available.

Target

The target used in the field tests is shown in Fig. 11. The reference was provided by the cat's-eye retroreflector in the upper left-hand corner. The retroreflector defocuses the returning beam to allow the desired reference-to-object beam-energy ratio of between 4 to 1 and 10 to 1. The target portion consists of five sections of alternating black strips and 3M Scotchlite strips of equal width. The spatial frequencies were 12.5, 25, 50, 100, and 200 cycles/m. Diffraction-limited resolution for the 36-cm telescope at 1 km range with coherent illumination is approximately 250 cycles/mm.

PRELIMINARY EXPERIMENTS

The various components were tested in preliminary experiments at NRL over a 30-m path in a light tunnel. A 25-cm-diameter telescope was used rather than the 36-cm-diameter telescope because of the difficulty of focusing the latter at close range. Results for a three-bar USAF resolution target with no turbulence along the path are shown in Figs. 12a and 12b. These showed that the conventional image could be resolved to the diffraction limit but the reconstructed hologram resolution was limited to half that. No means of improving the holographic resolution could be found, even when the effects of limited film resolution and of the thick beamsplitter were eliminated. For most cases this limitation in resolution was not important, since the resolution for the field tests was limited by other factors.

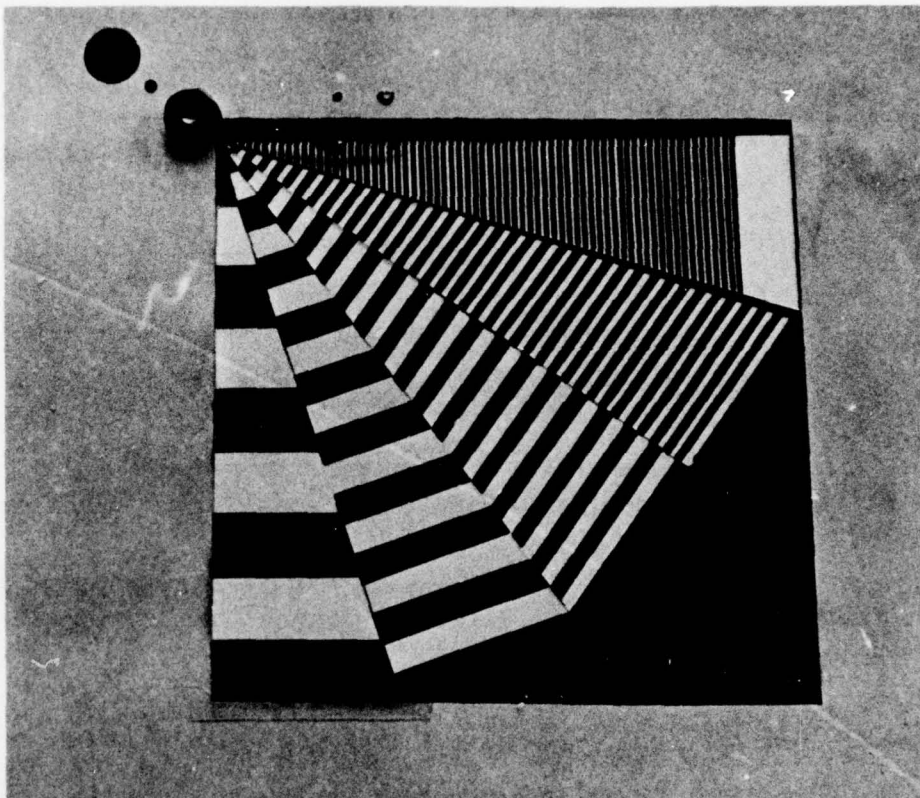
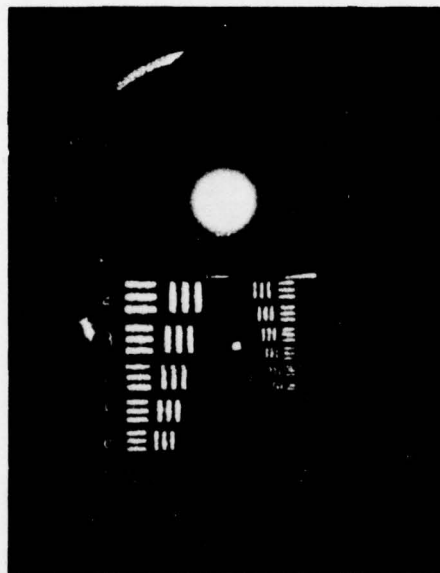


Fig. 11 — Retroreflective target used in the field tests

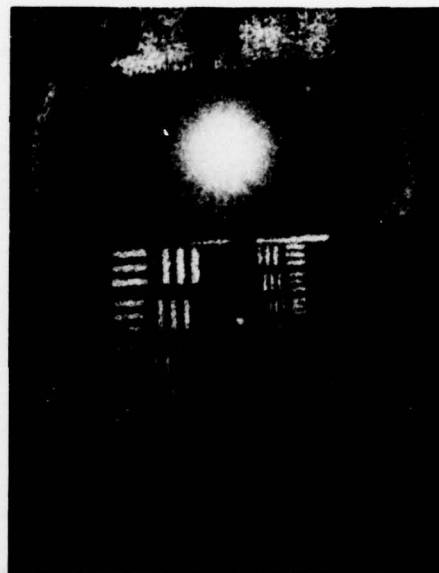
Localized turbulence was introduced with heaters placed 3 m in front of the telescope and directly below the path. The results are shown in Figs. 12c and 12d. The conventional image was degraded by a factor of 8 or greater in resolution, particularly for the horizontal bars, but the resolution of the holographic reconstruction was virtually unchanged, although there was some decrease in the signal-to-noise ratio. The resolution of the reconstruction was at least a factor of 4 better than the conventional image.

FIELD EXPERIMENTS

The field experiments were conducted at NRL's Chesapeake Bay Division over a 1-km range (Fig. 13). The 1-km range was chosen for safety, because it is well protected. It is immediately adjacent to the bay, running roughly parallel to the shore. All but the last portion of the path is over land, with the target being mounted about 2 m above the water level. The telescope, laser, and associated electronics were in a trailer at one end of the path. The laser beam was 20 cm from the optical axis of the telescope and 3 m above ground level.



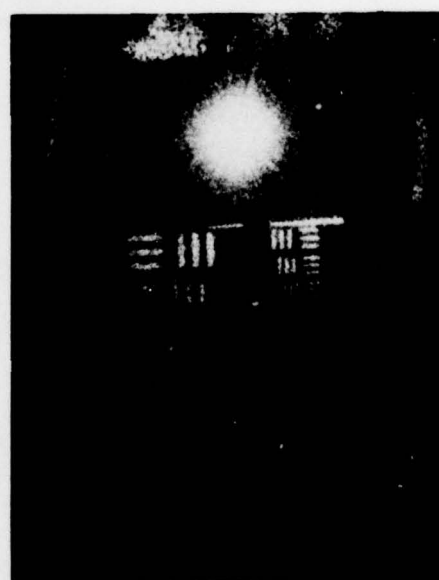
(a) Conventional image without turbulence



(b) Holographic image without turbulence



(c) Conventional image with turbulence



(d) Holographic image with turbulence

Fig. 12 — Results of preliminary tests in the laboratory, showing the comparison of the conventional and holographic images without and with turbulence

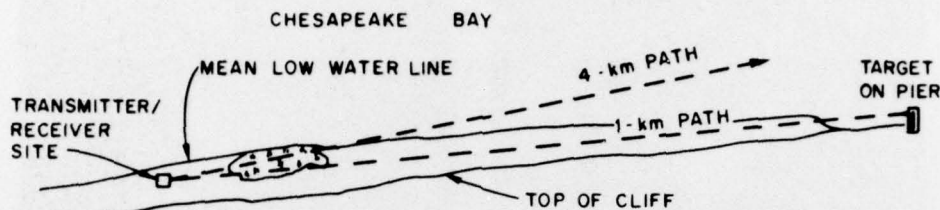


Fig. 13 — Test range at NRL's Chesapeake Bay Division

There were 257 shots on eight nights over the 1-km path from 23 October 1975 to 4 December 1975. During the series of tests the laser energy, pulse shape, and mode structure, were recorded for each shot. The holograms and conventional images were recorded on either Eastman 2496 or 2476 film. The trailer was kept open and unheated during runs in an attempt to avoid a turbulence layer at the receiver optics.

The laser beam pattern on the target was photographed on each shot from a range of 20 m, using Kodak 2485 film, with high speed and low resolution, or Kodak 2476 film, with medium speed and resolution. The pattern was photographed in an attempt to determine correlation between poor hologram reconstruction or conventional images and non-uniform target illumination.

No extensive meteorological instrumentation was available for this path. Only general weather conditions were recorded, and more detailed information on the turbulence would have been desirable.

RESULTS OF FIELD EXPERIMENTS

Figures 14a through 14e show some of the results obtained over the 1-km path. In the first pair of images (Fig. 14a) obtained on a night with low turbulence, both the holographic reconstruction and the conventional recording show resolution into the fourth group, which is nearly twice the diffraction limited value. The holographic reconstruction is noisier than the conventional image, as was the case in all of the tests. As discussed earlier, this noisiness could be improved with the use of higher contrast emulsion-and-developer combination. For this particular night with low turbulence, that would have been a good choice. However with more turbulence the dynamic range of the combination would be inadequate to record the intensity variations.

In Fig. 14b the holographic reconstruction is seen to give better resolution than the conventional image, in which not even the first group can be seen. Although the output of a Fabry-Perot etalon showed a second longitudinal laser mode, no effect can be seen on the reconstruction. For comparison, Fig. 14c, which was taken only 2 minutes after the preceeding shot, yielded no holographic reconstruction, but the conventional image has resolution into the first or second group. Only a single laser mode was observed. One cause for this reversal is the much more intense retroreflection observed in the conventional image, which tended to drive the hologram recording into saturation.

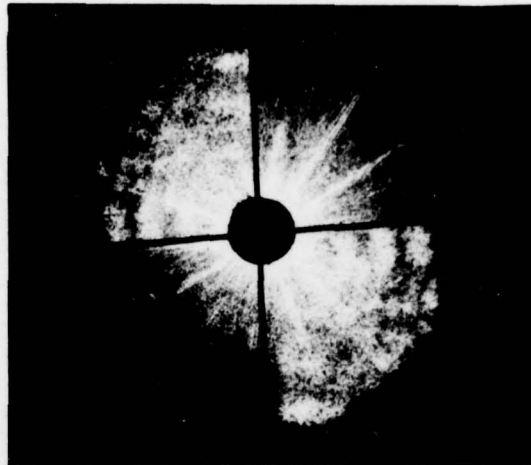
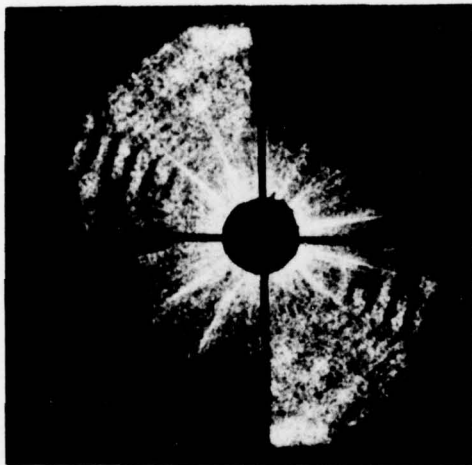


Fig. 14a — Simultaneous holographic image (top) and conventional image (bottom) of the target shown in Fig. 11 obtained over the 1-km path during low turbulence.

Fig. 14b — Typical pair of images obtained over the 1-km path

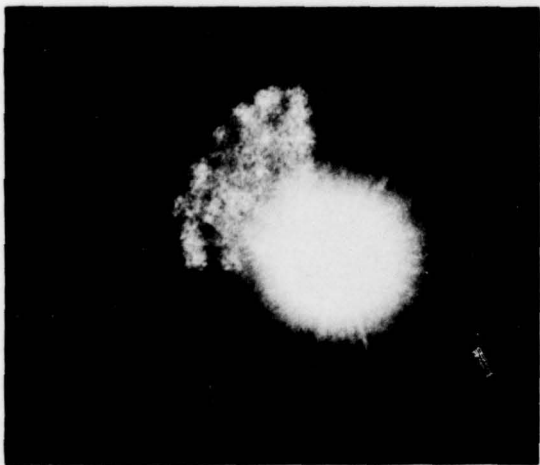
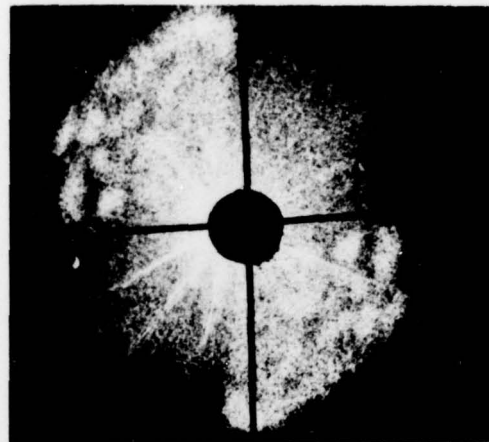
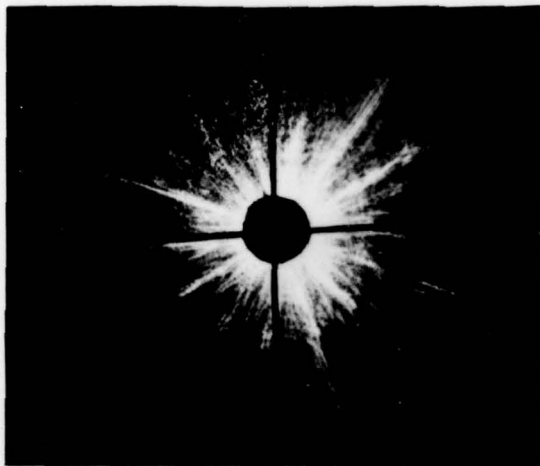


Fig. 14c — Pair of images obtained over the 1-km path when the retroreflection was intense

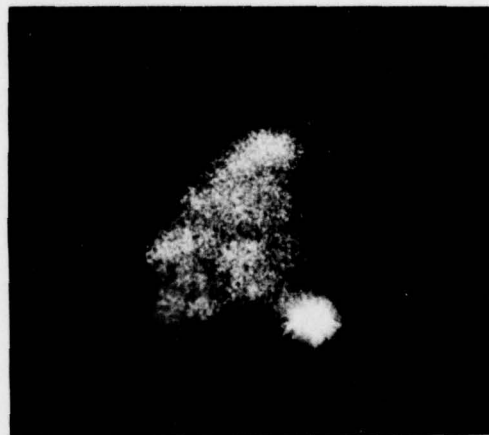


Fig. 14d — Selected pair of images obtained over the 1-km path showing better resolution by the holographic reconstruction

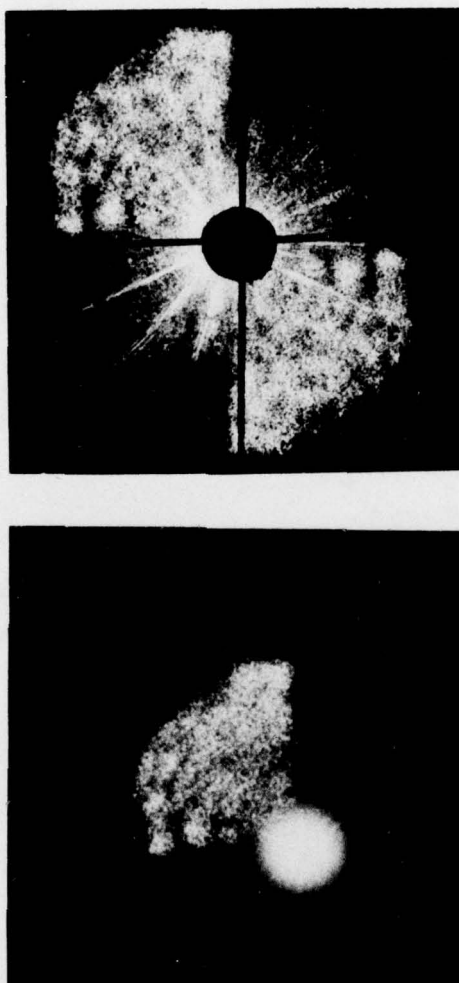


Fig. 14e — Selected pair of images obtained over the 1-km path showing equal or better resolution by the holographic reconstruction

Figures 14d and 14e show additional selected results. Although these images are not necessarily typical, in most cases the holographic reconstruction provided equal or somewhat better resolution, approaching a factor of 2, than the conventional image taken simultaneously. The holographic image provided poorer resolution when the retroreflector illumination was poor or when the reference beam return was nonuniform, which resulted in an effective hologram size considerably less than the reduced telescope aperture.

One additional test was performed at a 4-km range on an overwater path with a larger target. The data from this experiment indicate a beam breakup so severe than in many instances the retroreflector was not illuminated (Fig. 15b) and hence no hologram could

BLODGETT, EASTON, KONCEN



(a) At 1 km



(b) At 4 km

Fig. 15 — Typical laser illumination of the target a 1 km and a target at 4 km

be formed. In those instances when a return from the retroreflector was present, it was again severely broken up by the atmosphere, resulting in a greatly reduced effective hologram size. In all of these tests at the 4-km range the most that could be observed in either the holographic reconstruction or the conventional image was the general shape of the target.

CONCLUSIONS

These experiments on imaging through a horizontal terrestrial path indicate that although holographic imaging as opposed to conventional active coherent imaging shows some improvement in resolution, its use is not warranted in most circumstances. Its use is not warranted primarily because of the decreased signal-to-noise ratio and the presence of the twin image, which in some target configurations confuses the information in the reconstructed hologram. These problems may possibly be overcome by electronic imaging detectors which increase the dynamic range of the recorded hologram and by the local-reference-beam technique or a modification to provide a reliable reference source.

In the local-reference-beam technique [12] the reference wave required for forming the interference fringes of the hologram is derived from the light reflected from the object itself. In the original local-reference-beam demonstration the return beam from the object was divided using a beamsplitter, with one part focused to a small image of the object using a lens or curved mirror. This small image served as a "point source" for the reference beam required for the hologram and was recombined with the other portion of the object wave at the photographic emulsion. On reconstruction the hologram was illuminated with a true point source, but distortions resulted because the reconstruction beam did not duplicate the original reference wave. These distortions can be significantly reduced by using this technique to form an image-plane hologram [13]. In this case the object wave is focused on the hologram during recording while the reference beam is still a quasi point source formed by focusing the other portion of the object wave to a greatly reduced image of the original object. The advantage that the image-plane hologram offers is an insensitivity to reference source size; therefore high-resolution hologram reconstructions should be possible with this technique.

Employment of this technique for long-range holography would remove the dependence on the presence of a strong glint from the target and could make it possible to separate the twin images in the reconstruction by providing a spatial offset for the reference wave. Large variations in the intensity of the return across the receiving aperture however would still contribute to a decrease in the signal-to-noise ratio of the reconstruction. In addition an increase in the reference-wave offset angle would require a higher resolution film, which would generally be less sensitive.

REFERENCES

1. J.W. Goodman, W.H. Huntley, Jr., D.W. Jackson, and M. Lehmann, Appl. Phys. Lett. 8, 311 (1966).
2. Restoration of Atmospherically Degraded Images, Vols. 1 and 2, National Academy of Sciences, National Research Council, 1966.

BLODGETT, EASTON, KONCEN

3. J.D. Gaskill, J. Opt. Soc. Am. **58**, 600 (1968).
4. J.D. Gaskill, J. Opt. Soc. Am. **59**, 308 (1969).
5. I.N. Davydova and Yu.N. Denisyuk, Optics and Spectroscopy **26**, 450 (1969).
6. J.W. Goodman, D.W. Jackson, M. Lehmann, and J. Knotts, Appl. Optics **8**, 1581 (1969).
7. J.W. Goodman and M. Lehmann, "Detection Processes for Wavefront Reconstruction Receivers," Stanford Electronics Labs, 1967.
8. S. Yokozeki and T. Suzuki, Appl. Optics **11**, 446 (1972).
9. R.L. Easton, Jr., and J.A. Blodgett, "Characteristics of Some 35-mm Films for Holography at 694.3 nm," NRL Report 8142, September 12, 1977.
10. P.H. Deitz, Appl. Optics, **8**, 2293 (1969).
11. M. Levy, Photo Sci. and Engineering, **11**, 46, 1967.
12. H.J. Caulfield, Phys. Letters, **27A**, 319, 1968.
13. Gerald B. Brandt, Appl. Optics, **8**, 1421, 1969.

